



Wave Journal Bearings Under Dynamic Loads

Florin Dimofte
University of Toledo, Toledo, Ohio

Robert C. Hendricks
Glenn Research Center, Cleveland, Ohio

The NASA STI Program Office . . . in Profile

Since its founding, NASA has been dedicated to the advancement of aeronautics and space science. The NASA Scientific and Technical Information (STI) Program Office plays a key part in helping NASA maintain this important role.

The NASA STI Program Office is operated by Langley Research Center, the Lead Center for NASA's scientific and technical information. The NASA STI Program Office provides access to the NASA STI Database, the largest collection of aeronautical and space science STI in the world. The Program Office is also NASA's institutional mechanism for disseminating the results of its research and development activities. These results are published by NASA in the NASA STI Report Series, which includes the following report types:

- **TECHNICAL PUBLICATION.** Reports of completed research or a major significant phase of research that present the results of NASA programs and include extensive data or theoretical analysis. Includes compilations of significant scientific and technical data and information deemed to be of continuing reference value. NASA's counterpart of peer-reviewed formal professional papers but has less stringent limitations on manuscript length and extent of graphic presentations.
- **TECHNICAL MEMORANDUM.** Scientific and technical findings that are preliminary or of specialized interest, e.g., quick release reports, working papers, and bibliographies that contain minimal annotation. Does not contain extensive analysis.
- **CONTRACTOR REPORT.** Scientific and technical findings by NASA-sponsored contractors and grantees.

- **CONFERENCE PUBLICATION.** Collected papers from scientific and technical conferences, symposia, seminars, or other meetings sponsored or cosponsored by NASA.
- **SPECIAL PUBLICATION.** Scientific, technical, or historical information from NASA programs, projects, and missions, often concerned with subjects having substantial public interest.
- **TECHNICAL TRANSLATION.** English-language translations of foreign scientific and technical material pertinent to NASA's mission.

Specialized services that complement the STI Program Office's diverse offerings include creating custom thesauri, building customized data bases, organizing and publishing research results . . . even providing videos.

For more information about the NASA STI Program Office, see the following:

- Access the NASA STI Program Home Page at <http://www.sti.nasa.gov>
- E-mail your question via the Internet to help@sti.nasa.gov
- Fax your question to the NASA Access Help Desk at 301-621-0134
- Telephone the NASA Access Help Desk at 301-621-0390
- Write to:
NASA Access Help Desk
NASA Center for Aerospace Information
7121 Standard Drive
Hanover, MD 21076



Wave Journal Bearings Under Dynamic Loads

Florin Dimofte
University of Toledo, Toledo, Ohio

Robert C. Hendricks
Glenn Research Center, Cleveland, Ohio

Prepared for the
56th Annual Meeting and Exhibit
sponsored by the Society of Tribology and Lubrication Engineers
Orlando, Florida, May 20–24, 2001

National Aeronautics and
Space Administration

Glenn Research Center

Acknowledgments

This work was performed under NASA NCC3-436 at NASA Glenn Research Center in Cleveland, Ohio. The authors would like to express their gratitude to Mr. Joseph Hemminger for continued interest and support.

Available from

NASA Center for Aerospace Information
7121 Standard Drive
Hanover, MD 21076

National Technical Information Service
5285 Port Royal Road
Springfield, VA 22100

Available electronically at <http://gltrs.grc.nasa.gov/GLTRS>

WAVE JOURNAL BEARINGS UNDER DYNAMIC LOADS

Florin Dimofte
University of Toledo
Toledo, Ohio 43606

Robert C. Hendricks
National Aeronautics and Space Administration
Glenn Research Center
Cleveland, Ohio 44135

SUMMARY

The dynamic behavior of the wave journal bearing was determined by running a three-wave bearing with an eccentrically mounted shaft. A transient analysis was developed and used to predict numerical data for the experimental cases. The three-wave journal bearing ran stably under dynamic loads with orbits well inside the bearing clearance. The orbits were almost circular and nearly free of the influence of, but dynamically dependent on, bearing wave shape.

Experimental observations for both the absolute bearing-housing-center orbits and the relative bearing-housing-center-to-shaft-center orbits agreed well with the predictions. Moreover, the subsynchronous whirl motion generated by the fluid film was found experimentally and predicted theoretically for certain speeds.

SYMBOLS

B	damping coefficient between bearing housing and its support, N·s/m
$B_{ij}(i = r, t; j = r, t)$	film damping coefficients, N·s/m
C	bearing radial clearance, m
F_r, F_t	fluid film force components along and perpendicular to line of centers $O_1 - O$ (fig. 1), N
$F_{i0}(i = r, t)$	steady-state fluid film force components along and perpendicular to line of centers $O_1 - O$, N
F_ζ, F_η	fluid film force components along and perpendicular to line $O_0 - O$ (fig. 1), N
h	fluid film thickness, m
K	stiffness coefficient between bearing housing and its support, N/m
$K_{ij}(i = r, t; j = r, t)$	film stiffness coefficients, N/m
M	bearing-housing total mass, kg
O	bearing-housing center (fig. 1)
O_0	fixed center of rotation (fig. 1)
O_1	shaft center (fig. 1)
p	fluid film pressure, Pa
R	shaft radius (bearing normal radius), m
r	coordinate along line of centers
S	space (displacement) between shaft center O_1 and bearing-housing center O , m
$S_i(i = r, t)$	S components along and perpendicular to line of centers $O_1 - O$, m
t	time, s; coordinate perpendicular to line of centers
V	velocity between shaft center O_1 and bearing-housing center O , m/s

$V_{i(i=r,t)}$	V components along and perpendicular to line of centers $O_1 - O$, m/s
V_n	difference between shaft surface and bearing surface speed projected on perpendicular direction to shaft surface, m/s
V_θ	component of shaft surface speed along its circumference, m/s
z	axial coordinate parallel to shaft axis
ε	bearing eccentricity relative to shaft (relative movement) (fig. 1), $O_1 - O$, m, also bearing line of centers
ε/C	bearing sleeve-to-shaft eccentricity ratio
ε_0	bearing run-out (absolute movement) (fig. 1), $O_0 - O$, m
ε_0/C	bearing-housing absolute eccentricity ratio, $\varepsilon_0 = O_0 - O$
ζ, η	axes along and perpendicular to direction $O_0 - O$ (fig. 1)
θ	angular coordinate along shaft circumference, rad
μ	fluid film dynamic viscosity, N·s/m ²
ρ	fixed shaft run-out (fig. 1), $O_0 - O_1$, m
φ	angle between line of centers $O_1 - O$ and $O_0 - O$ (fig. 1), rad
ψ	rotation angle of $O_0 - O$ around O_0 (fig. 1), rad
Ω	rotation angle of $O_0 - O_1$ around O_0 (fig. 1), ωt , rad
ω	angular rotation speed (fig. 1), rad/s

INTRODUCTION

The wave bearing concept has been under development since 1992. Thus, the steady-state and dynamic performance under fixed side load (refs. 1 and 2) and the influence of both the number of waves and the ratio of wave amplitude to radial clearance (refs. 3 and 4) have been analyzed. Moreover, the steady-state characteristics of the wave journal bearing and its dynamic stability have been experimentally measured. Good agreement was found between the experimental data and theoretical predictions (refs. 5 to 8). In addition, the experimental work revealed good dynamic behavior of the wave bearing when subsynchronous whirl motion occurred. The wave bearing performed well, keeping the orbit of the subsynchronous motion inside the bearing clearance (refs. 7 and 8). Consequently, the wave bearing should perform well under the dynamic loading conditions that often occur in most rotating machinery. Any rotor can be subject to a dynamic load caused by an unbalance, or a run-out, of the shaft. This dynamic load is a rotating load that has a rotational speed equal to the rotor speed. Such a load can be simulated by running the bearing with a shaft that has a fixed run-out. Therefore, a transient analysis was performed to predict bearing behavior under a rotating load. Then an experiment was conducted to record the orbits of the bearing-housing center when the shaft has a known fixed run-out.

ANALYSIS

Bearing-housing-center movement can be studied by using the motion equation of the center along and perpendicular to the radial direction $O_0 - O$ (axes ζ and η in fig. 1):

$$MC \left[\frac{d^2 \epsilon_0}{dt^2} - \epsilon_0 \left(\frac{d\psi}{dt} \right)^2 \right] + K\epsilon_0 + B \frac{d\epsilon_0}{dt} = F_\zeta \quad (1)$$

$$MC \left(\epsilon_0 \frac{d^2 \psi}{dt^2} + 2 \frac{d\psi}{dt} \frac{d\epsilon_0}{dt} \right) + K\epsilon_0 \psi + B\epsilon_0 \frac{d\psi}{dt} = F_\eta$$

Also, figure 1 shows that the eccentricity $\epsilon = O_1 - O$ (where $O_1 - O$ is the line joining the shaft center O_1 and the bearing-housing center O) and that the shaft run-out $\rho = O_0 - O_1$. Assuming that the motion starts from the downward vertical where the shaft and the bearing are concentric ($\epsilon = 0$), when the shaft rotates around O_0 with the angular speed ω , ρ makes the angle Ω and drives the bearing so that ϵ_0 makes the angle ψ .

The governing equations (1) are two scalar, coupled, nonlinear ordinary differential equations. These equations are integrated simultaneously by using a fourth-order Runge-Kutta method for known values of M , C , F_ζ , F_η , K , and B and initial values of ϵ_0 , ψ , $d\epsilon_0/dt$, and $d\psi/dt$ (ref. 9). The fluid film forces applied to the bearing surface are

$$F_\zeta = F_r \cos \phi + F_t \sin \phi \quad (2)$$

$$F_\eta = F_r \sin \phi - F_t \cos \phi$$

The projections of fluid film force along and perpendicular to the line of centers are

$$F_r = F_{r_0} + K_{rr}S_r + K_{rt}S_t + B_{rr}V_r + B_{rt}V_t \quad (3)$$

$$F_t = F_{t_0} + K_{tr}S_r + K_{tt}S_t + B_{tr}V_r + B_{tt}V_t$$

The bearing steady-state force and dynamic stiffness and damping coefficients can be computed by integrating the Reynolds pressure equation at each time step location of the shaft with respect to the bearing. This equation, assuming the gas will expand isothermally, is

$$\frac{\partial}{R\partial\theta} \left(\frac{h^3}{\mu} p \frac{\partial p}{R\partial\theta} \right) + \frac{\partial}{\partial z} \left(\frac{h^3}{\mu} p \frac{\partial p}{\partial z} \right) = 6 \left[2pV_n + 2 \frac{\partial(ph)}{\partial t} + pV_\theta \frac{\partial h}{R\partial\theta} + h \frac{\partial(pV_\theta)}{R\partial\theta} \right] \quad (4)$$

The Reynolds equation (4) can be integrated by using its complex form and a small perturbation technique. This procedure is described, for instance, in reference 10.

The solution procedure can start with an input data set (bearing length, diameter, radial clearance, shaft turning speed, shaft run-out, and the time step). In addition, a set of starting values at time = 0 are required:

$$\epsilon_0 = \rho, \quad \frac{\partial \epsilon_0}{\partial t} = 0 \quad (5)$$

$$\psi = 0, \quad \frac{\partial \psi}{\partial t} = 0$$

Then, at each time step, where ϵ_0 , ψ , and Ω ($\Omega = \omega t$) are known, the O_0O_1O triangle (fig. 1) is known, and all geometrical parameters as well as displacements and velocities can be calculated. Therefore, the Reynolds equation (4) can be integrated over the fluid film. Then, all parameters of the motion equation (1) are known as well as the starting values for the next time step (ϵ_0 , ψ , and their time derivatives Ω). The procedure is repeated until the orbits are completed.

APPARATUS

The wave bearing rig described in references 5 to 8 was used to perform the experimental work. The axis of the spindle that drives this rig is vertical, and the experimental bearing housing is mounted on the rig table and supported by two pressurized thrust plates. This configuration keeps the bearing housing stiff in the axial and angular directions but allows it to move freely in the radial direction. The experimental shaft is an extension of the rig spindle shaft. It is mounted into the tapered end of the spindle shaft with a fixed run-out (for this experiment $11 \pm 0.1 \mu\text{m}$). A cross section by a horizontal plane of the experimental bearing is shown in figure 2. The fixed rotation center for the system is O_0 . The centers of the shaft and the bearing housing are O_1 and O , respectively. The shaft run-out $O_0 - O_1$ is fixed.

The goal of this work was to record and predict the absolute and relative orbits of the bearing-housing center O . The motion of the center O can be observed like an absolute motion for instance with regard to the center of rotation O_0 or like a relative motion with regard to the center of the shaft O_1 . Figure 3 shows the experimental bearing setup. Two sets of light-beam proximity probes were used. Two probes were located at 90° in the bottom side of the bearing housing and “looking” at the shaft. These probes detected the orbit of the bearing-housing center relative to the shaft center ($O - O_1$). The second set of two probes were located also at 90° but held by supports fixed on the rig table and “looking” at the bearing housing. These latter probes detected the absolute orbit of the bearing-housing center ($O - O_0$). A polished circumferential strip was made on the outside bearing-housing surface to avoid asperity noise from its roughness. The light-beam probes were calibrated by using the known fixed run-out of the shaft. The displacement of the shaft was measured with a precision of $0.1 \mu\text{m}$. The theoretical predictions of the orbits were made through a transient analysis of the bearing-housing-center motion.

RESULTS AND DISCUSSION

The experimental bearing was $51 \pm 0.01 \text{ mm}$ in diameter, $58 \pm 0.01 \text{ mm}$ in length, $20 \pm 1 \mu\text{m}$ in radial clearance, and $2.2 \pm 0.01 \text{ kg}$ in mass. The bearing had three waves with a 0.5 ± 0.07 ratio of wave amplitude to radial clearance. The shaft was set with an $11 \pm 0.1 \mu\text{m}$ run-out. The damping, B in eqs. (1), in the bearing-housing support and connection system was found to be $0.05 \text{ N}\cdot\text{s}/\text{m}$. The stiffness, K in eqs. (1), had little influence on the bearing orbits and was approximately zero. The top proximity probes (fig. 3) produced 500 mV for 5.78- and 4.78- μm displacements in the horizontal and vertical directions, respectively, and the bottom probes produced 500 mV for 6.11- and 6.90- μm displacements in the horizontal and vertical directions, respectively. (Horizontal and vertical directions refer to the directions on the oscilloscope photographs shown on the right sides of figures 4 and 5, 90° apart in the physical plane.)

The test rig was run at four speeds up to 5540 rpm. Below 3100 rpm both the observed and predicted orbits of the bearing-housing center showed that a subsynchronous whirl motion took place inside the bearing clearance. Figure 4 shows both the predicted and observed orbits for relative and absolute motion of the bearing-housing center when the shaft rotated at 2156 rpm. When the speed increased above 3100 rpm, the motion stabilized, as shown in figure 5 for a shaft speed of 5539 rpm.

Both the absolute and relative observed orbits of the bearing-housing center are shown as oscilloscope photographs on the right sides of figures 4 and 5. On the left sides of these figures the computed orbits are presented with a time step of 0.000001 s ($10 \mu\text{s}$) and for 30 000 steps. The experimental orbits appeared as ellipses rather than circles because of the difference in the probe sensitivity in the horizontal and vertical directions mentioned above. Both experimental orbits in figure 4 have a specific pattern caused by subsynchronous whirl motion. The transient analysis also revealed this pattern. Both the experimental and theoretical absolute orbits (fig. 4(a)) were within a radius of 5 to $12 \mu\text{m}$. Both the experimental and theoretical relative orbits (fig. 4(b)) were within a radius of approximately $5 \mu\text{m}$.

The bearing stability increased as the running speed of the rig increased. Figure 5 shows the results for 5539 rpm. The experimental orbits were perfectly stable. The shaft run-out made large absolute orbits of the bearing housing (right side of fig. 5(a)). However, the radius of the relative orbits was approximately $2.5 \mu\text{m}$ (right side of fig. 5(b)) despite the $11 \pm 0.1 \mu\text{m}$ shaft run-out (i.e., the bearing followed the shaft very well). The predicted orbits, shown on the left side of figure 5, matched very well with the observed orbits. The theory also showed that the bearing would run stably. After a couple of rotations from the starting point the orbits were stable, keeping almost the same path.

The relative orbits of the bearing housing increased but the absolute orbits decreased as the speed increased. This effect showed the influence of both external damping and bearing inertia on the magnitude of orbit radius. In addition, the bearing actually ran more and more stably as speed increased, and the theory showed that the number of rotations before the bearing reached a stable orbit would diminish as speed increased.

All runs showed only a small influence of the bearing wave shape on the orbit shape despite the experimental bearing's large wave amplitude ratio, 0.5 ± 0.07 . This result confirmed that a wave bearing with few waves, such as three, worked well under dynamic loads. The bearing behaved in such a way as to average the influence of the waves.

Two types of shaft-centered motion can be defined with respect to the center of the bearing: (i) stable unbalance or run-out orbits (e.g., fig. 5(b)), where the center of unbalance rotates at shaft frequency; and (ii) fluid-film-induced unstable whirl orbits (e.g., fig. 4(b)) that are superimposed over the stable unbalance or run-out orbits at a specific frequency different from the rotation frequency. The unbalance motion (i) is seen in each graph, but the unstable whirl (ii) occurs only at specific rotational speeds.

CONCLUSIONS

The dynamic behavior of the wave journal bearing was determined by running a three-wave bearing with an eccentrically mounted shaft. The following conclusions were reached:

1. A dynamically loaded three-wave journal bearing can run stably, averaging its behavior when the wave exposure to the load is changing. The orbit radius of the relative motion between the shaft and the sleeve is smaller than the bearing clearance, and the motion is contained within the bearing clearance. The orbits are almost circular and nearly free of, but dynamically dependent on, the influence of bearing wave shape.
2. Good agreement between experimentally observed and theoretically predicted orbits was found at all tested speeds for both relative and absolute motions.
3. The subsynchronous whirl motion influences the bearing-housing-center orbits if the bearing speeds are in the region where the bearing itself is susceptible to subsynchronous whirl instability. When the bearing runs under such circumstances, the orbits show a specific pattern. This pattern was observed experimentally and was also confirmed theoretically by the transient analysis.

REFERENCES

1. Dimofte, F.: Wave Journal Bearing With Compressible Lubricant; Part I: The Wave Bearing Concept and a Comparison to the Plain Circular Bearing. *Tribol. Trans.*, vol. 38, no. 1, 1995, pp. 153–160.
2. Dimofte, F.: Wave Journal Bearing With Compressible Lubricant; Part II: A Comparison of the Wave Bearing With a Wave-Groove Bearing and a Lobe Bearing. *Tribol. Trans.*, vol. 38, no. 2, 1995, pp. 364–372.
3. Dimofte, F.: A Waved Journal Bearing Concept—Evaluating Steady-State and Dynamic Performance With a Potential Active Control Alternative. *Proceedings of the ASME 14th Biennial Conference on Mechanical Vibration and Noise*, DE-vol. 60, Vibration of Rotating Systems, ASME, NY, 1993, pp. 121–128.
4. Dimofte, F.: A Waved Journal Bearing Concept With Improved Steady-State and Dynamic Performance. *Rotordynamic Instability Problems in High-Performance Turbomachinery*, NASA CP-3239, 1993, pp. 419–429.
5. Dimofte, F.; and Addy, H.E.: Pressure Measurements of a Three Wave Journal Air Bearing. *Seals Flow Code Development—93*, NASA CP-10136, 1993, pp. 285–294.
6. Dimofte, F.; Addy, H.E.; and Walker, J.F.: Preliminary Experimental Results of a Three Wave Journal Air Bearing. *Advanced Earth-to-Orbit Propulsion Technology—1994*, R.J. Richmond and S.T. Wu, eds., NASA CP-3282, Vol. II, 1994, pp. 375–384.
7. Dimofte, F.; and Hendricks, R.C.: Fractional Whirl Motion in Wave Journal Bearings. *Seals Flow Code Development—95*, NASA CP-10181, 1995, pp. 337–340.
8. Dimofte, F.; and Hendricks, R.C.: Two- and Three-Wave Journal Bearing Fractional Whirl Motion. *Proceedings of The Society of Engineering Science 32nd Annual Technical Meeting*, 1995, pp. 773–774.
9. Vijayaraghavan, D.; and Brewe, D.: Frequency Effects on the Stability of a Journal Bearing for Periodic Loading. *J. Tribol.*, vol. 114, no. 1, 1992, pp. 107–115.
10. Dimofte, F.: Effect of Fluid Compressibility on Journal Bearing Performance. *Tribol. Trans.*, vol. 36, no. 3, 1993, pp. 341–350.

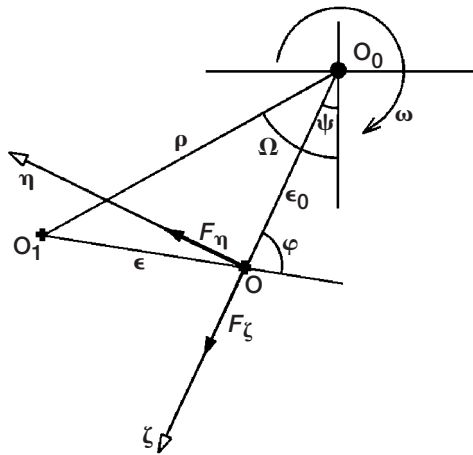


Figure 1.—Geometry of three-wave journal bearing. Rotation center, O_0 ; shaft center, O_1 ; and bearing-housing center, O .

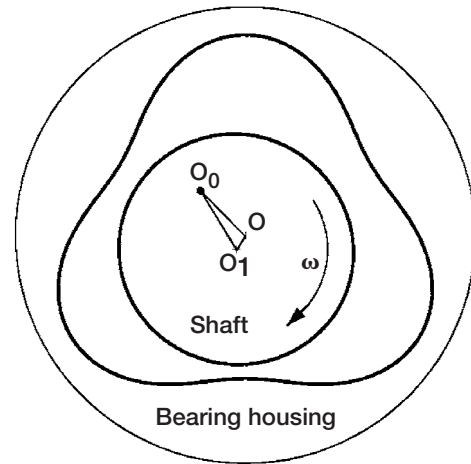


Figure 2.—Cross section of three-wave journal bearing by horizontal plane.

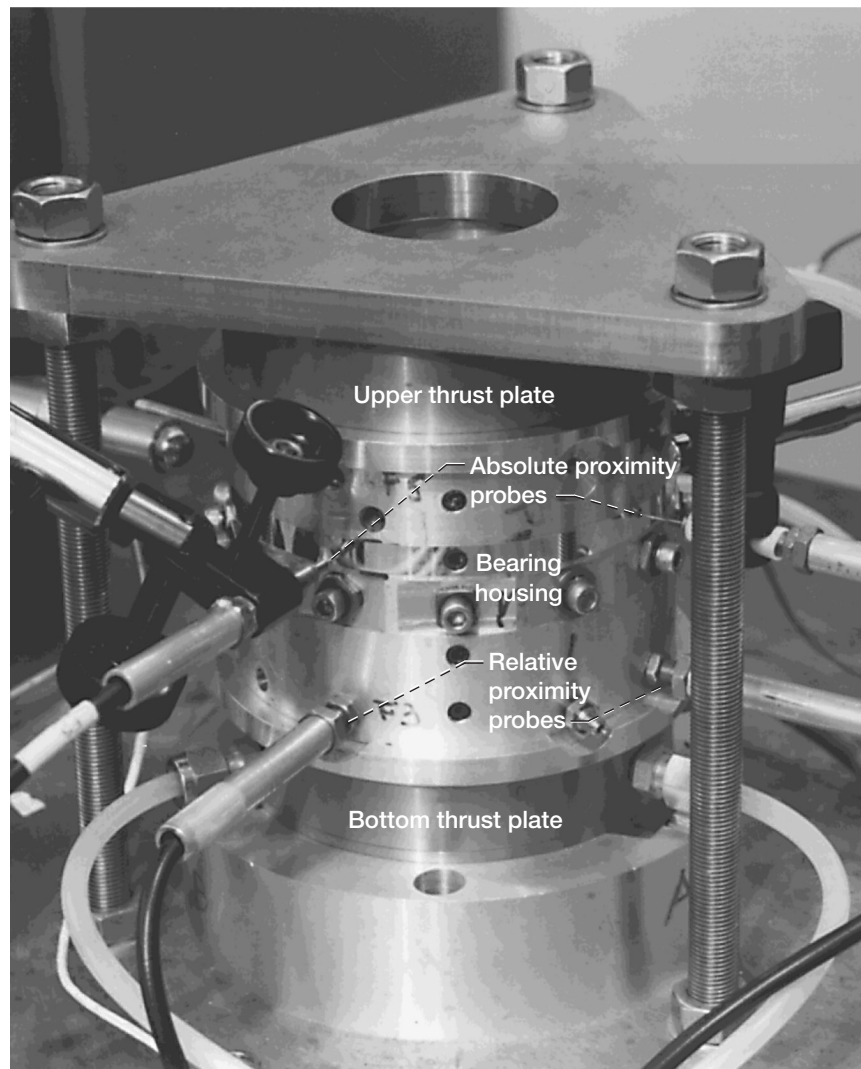


Figure 3.—Experimental bearing setup.

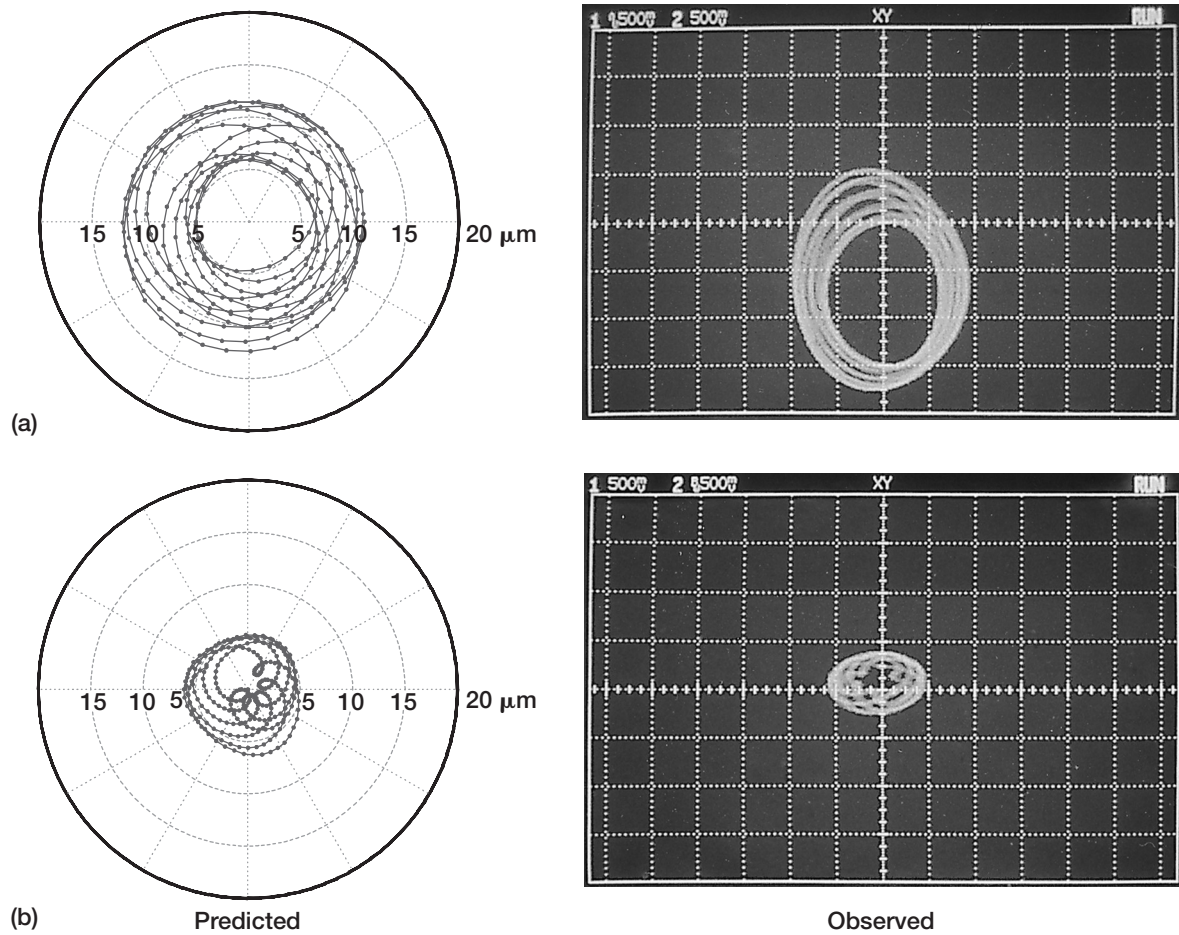
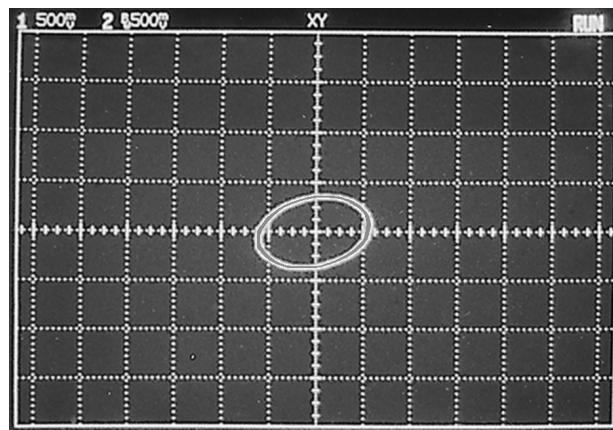
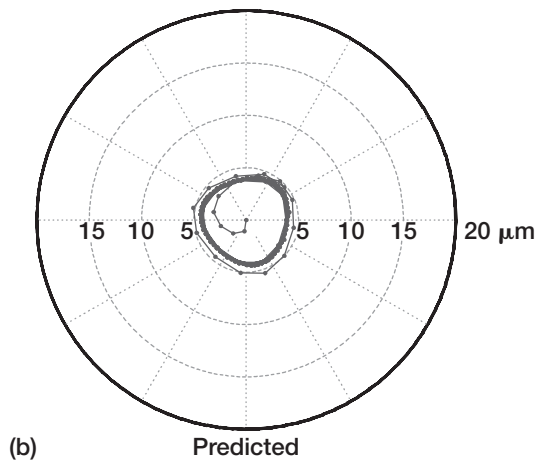
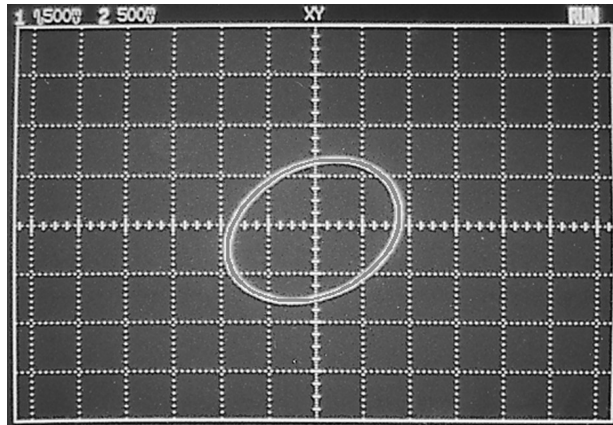
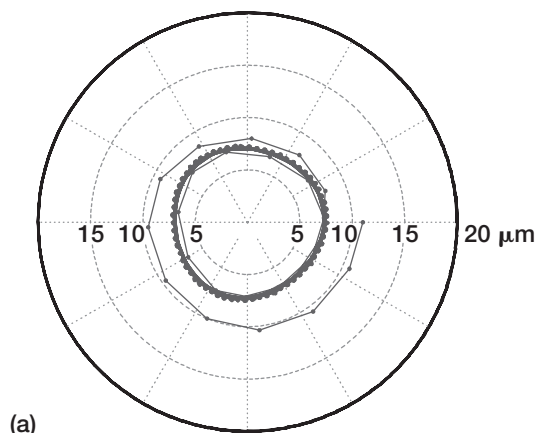


Figure 4.—Predicted and experimentally observed orbits of three-wave journal bearing at 2156-rpm shaft rotating speed. (a) Absolute bearing-housing-center orbits. (b) Relative bearing-housing-center-to-shaft-center orbits.



Observed

Figure 5.—Predicted and experimentally observed orbits of three-wave journal bearing at 5539-rpm shaft rotating speed. (a) Absolute bearing-housing-center orbits. (b) Relative bearing-housing-center-to-shaft-center orbits.

REPORT DOCUMENTATION PAGE			Form Approved OMB No. 0704-0188	
Public reporting burden for this collection of information is estimated to average 1 hour per response, including the time for reviewing instructions, searching existing data sources, gathering and maintaining the data needed, and completing and reviewing the collection of information. Send comments regarding this burden estimate or any other aspect of this collection of information, including suggestions for reducing this burden, to Washington Headquarters Services, Directorate for Information Operations and Reports, 1215 Jefferson Davis Highway, Suite 1204, Arlington, VA 22202-4302, and to the Office of Management and Budget, Paperwork Reduction Project (0704-0188), Washington, DC 20503.				
1. AGENCY USE ONLY (Leave blank)		2. REPORT DATE February 2002		3. REPORT TYPE AND DATES COVERED Technical Memorandum
4. TITLE AND SUBTITLE Wave Journal Bearings Under Dynamic Loads			5. FUNDING NUMBERS WU-712-30-13-00	
6. AUTHOR(S) Florin Dimofte and Robert C. Hendricks				
7. PERFORMING ORGANIZATION NAME(S) AND ADDRESS(ES) National Aeronautics and Space Administration John H. Glenn Research Center at Lewis Field Cleveland, Ohio 44135-3191			8. PERFORMING ORGANIZATION REPORT NUMBER E-12918	
9. SPONSORING/MONITORING AGENCY NAME(S) AND ADDRESS(ES) National Aeronautics and Space Administration Washington, DC 20546-0001			10. SPONSORING/MONITORING AGENCY REPORT NUMBER NASA TM-2002-211079	
11. SUPPLEMENTARY NOTES Prepared for the 56th Annual Meeting and Exhibit sponsored by the Society of Tribology and Lubrication Engineers, Orlando, Florida, May 20-24, 2001. Florin Dimofte, University of Toledo, 2801 W. Bancroft Street, Toledo, Ohio 43606, under NCC3-436 and Robert C. Hendricks, NASA Glenn Research Center. Responsible person, Robert C. Hendricks, organization code 5000, 216-977-7507.				
12a. DISTRIBUTION/AVAILABILITY STATEMENT Unclassified - Unlimited Subject Categories: 37 and 64 Available electronically at http://gltrs.grc.nasa.gov/GLTRS This publication is available from the NASA Center for AeroSpace Information, 301-621-0390.			12b. DISTRIBUTION CODE	
13. ABSTRACT (Maximum 200 words) The dynamic behavior of the wave journal bearing was determined by running a three-wave bearing with an eccentrically mounted shaft. A transient analysis was developed and used to predict numerical data for the experimental cases. The three-wave journal bearing ran stably under dynamic loads with orbits well inside the bearing clearance. The orbits were almost circular and nearly free of the influence of, but dynamically dependent on, bearing wave shape. Experimental observations for both the absolute bearing-housing-center orbits and the relative bearing-housing-center-to-shaft-center orbits agreed well with the predictions. Moreover, the subsynchronous whirl motion generated by the fluid film was found experimentally and predicted theoretically for certain speeds.				
14. SUBJECT TERMS Dynamic load; Gas bearing; Wave bearing; Dynamics; Journal bearing			15. NUMBER OF PAGES 14	
			16. PRICE CODE	
17. SECURITY CLASSIFICATION OF REPORT Unclassified	18. SECURITY CLASSIFICATION OF THIS PAGE Unclassified	19. SECURITY CLASSIFICATION OF ABSTRACT Unclassified	20. LIMITATION OF ABSTRACT	